Analysis of Dielectric Resonator Cavities Using the Finite Integration Technique

JOVAN E. LEBARIC, MEMBER, IEEE, AND DARKO KAJFEZ, SENIOR MEMBER, IEEE

Abstract — **Resonant modes in shielded dielectric resonators are studied by a numerical technique which yields the resonant frequencies, modal field distribution, and Q factors of various resonant modes, including the hybrid modes. The technique employs field discretization by virtue of dual electric and magnetic grids and allows for a direct numerical solution of the integral form of Maxwell's equations for specified boundary conditions. The details of the matrix formulation are explained on an example of the cavity subdivided into a grid consisting of 3×3 electric cells. A modal field plot exhibiting a spiraling behavior has been observed.**

I. Introduction

RIGOROUS NUMERICAL solutions for the electromagnetic field inside resonant cavities containing dielectric resonators have traditionally been obtained by the mode-matching procedures, and more recently, by the finite-element procedures. A review of most frequently used procedures can be found in [1]. The present paper will describe an alternative procedure, called the finite integration technique (FIT), which is particularly convenient when the cavity volume is filled with inhomogeneous dielectrics. The procedure has a similarity to a finite difference method, such as that used in [2], but has the advantage that the interface between different dielectric media does not require any special programming considerations.

The FIT is a numerical technique for direct solution of Maxwell's equations [3]–[6]. The technique is based on the integral form of Maxwell's equations for time-harmonic electromagnetic fields in lossless linear media:

$$\oint \vec{E} \cdot d\vec{l} = -j\omega \iint \vec{B} \cdot d\vec{s} \tag{1}$$

$$\oint \vec{H} \cdot d\vec{l} = j\omega \iint \vec{D} \cdot d\vec{s} \tag{2}$$

$$\oiint \vec{D} \cdot d\vec{s} = 0 \tag{3}$$

$$\oiint \vec{B} \cdot d\vec{s} = 0 \tag{4}$$

Manuscript received January 17, 1989; revised May 25, 1989. This work was supported in part by the National Science Foundation under Grant ECS-8443558, including the use of the Cray XMP-48 Supercomputer at NCSA, Champaign, IL.

J. E. Lebaric is with the Rose–Hulman Institute of Technology, Terre Haute, IN 47803.

D. Kajfez is with the Department of Electrical Engineering, University of Mississippi, University, MS 38677.

IEEE Log Number 8930516.

supplemented by the constitutive relationships:

$$\vec{D} = \epsilon \vec{E} \tag{5}$$

$$\vec{B} = \mu \vec{H}. \tag{6}$$

The permittivity ϵ and the permeability μ of linear, isotropic media are scalar functions of position. The equations (1) to (6), subject to the perfect-electric-conductor boundary conditions, constitute the boundary value problem to be solved numerically, for the specified geometry and media distribution. Extensions to domains with small media and wall losses can be made using standard perturbational techniques [7].

This paper describes the systematic discretization of Maxwell's equations which leads, for source-free domains involving isotropic media, to an equivalent standard algebraic eigenvalue problem. The FIT solution is inherently free of nonphysical, "spurious" modes, known to plague the finite element solutions [8], since the divergence equations are incorporated into the eigenvalue problem formulation from the onset.

As the resonant frequencies of the lossless cavity are obtained from the real eigenvalues, arranged in ascending order, there is no danger of overlooking one of them. In the mode-matching technique, it is known that some of the resonant frequencies may be overlooked, if the complex modes are not included [9].

An important convenience of the FIT is the freedom of rearranging the distribution of dielectric materials within the cavity by simply modifying the input data of the computer program.

II. Volume and Field Discretization

The simultaneous volume and field discretization is specifically tailored for Maxwell's equations by defining "dual" electric and magnetic grids. The use of dual grids [10] provides for the coupling of the electric and magnetic fields, expressed by the curl equations of Maxwell.

The cylindrical coordinate system (r, ϕ, z) is a natural choice for problems with rotational symmetry, noting that this property implies here not only the rotational symmetry of the problem geometry but also the invariance of media parameters with the angle of azimuth ϕ. Fig. 1 illustrates two adjacent elementary volume cells, one electric and one magnetic, and their respective field nodes. The

0018-9480/89/1100-1740$01.00

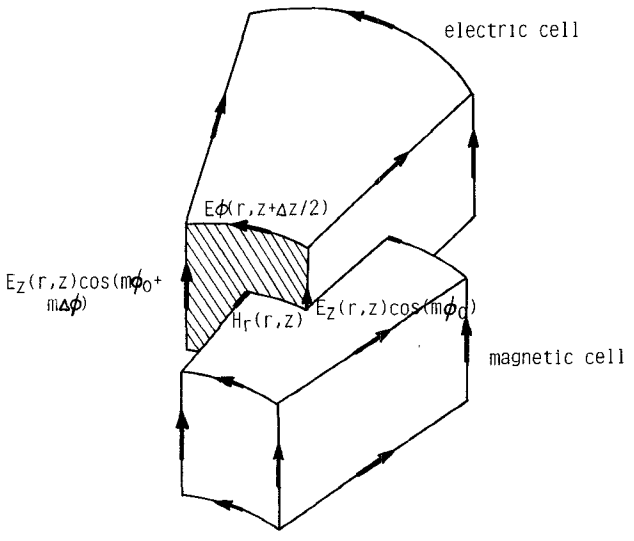

Fig. 1. Relative position of an adjacent electric and magnetic cell.

two cells, each representing its respective grid, are spatially shifted by $\Delta r/2$, $\Delta\phi/2$, and $\Delta z/2$. The permittivity ϵ is considered constant within an electric cell, but may vary from one electric cell to another in an arbitrary manner.

Field components are assigned to field nodes, residing at the centers of their respective cell sides: electric field components to the electric cells and magnetic field components to the magnetic cells. All nodal field components, as evident from Fig. 1, must have one of the three coordinate directions, that is, must be r-directed, ϕ-directed, or z-directed. The electric and magnetic fields are thus, by virtue of dual grids, simultaneously "sampled" and resolved into their orthogonal components. Also, the continuity of tangential field components across the dielectric interface is automatically imposed because the field components are shared by the adjacent volume cell, which may represent a different medium.

III. Modal Expansion

A three-dimensional interior electromagnetic boundary value problem with rotational symmetry can be reduced to an equivalent two-dimensional problem using Fourier series expansion with respect to the angle of azimuth ϕ. Linear combination of harmonic functions must be used for anisotropic media to accommodate the coupling of "degenerate" modes [11], while it is sufficient to use only one harmonic function, either sine or cosine, for isotropic media and uniaxial anisotropic media. For the later two the solution may be written as [5]

$$\vec{E}(r,\phi,z)=\sum_{m=0}^{\infty}\left[\hat{r}E_{mr}(r,z)\cos(m\phi)+\hat{\phi}E_{m\phi}(r,z)\sin(m\phi)+\hat{z}E_{mz}(r,z)\cos(m\phi)\right] \quad (7)$$

$$\vec{H}(r,\phi,z)=\sum_{m=0}\left[\hat{r}H_{mr}(r,z)\sin(m\phi)+\hat{\phi}H_{m\phi}(r,z)\cos(m\phi)+\hat{z}H_{mz}(r,z)\sin(m\phi)\right]. \quad (8)$$

The above expansion is referred to as the modal expansion and the integer m is referred to as the mode index. The main benefit of this expansion is the ability to integrate analytically with respect to the angle of azimuth ϕ and thus reduce the original three-dimensional problem to an equivalent two-dimensional problem.

IV. Discretization of Curl and Divergence Equations

The integral forms of the curl equations of Maxwell (1) and (2) involve line integrals of $\vec{E}$ and $\vec{H}$ and surface integrals of $\vec{B}$ and $\vec{D}$. The surface of integration is a cell face, its circumference being the contour of integration for the corresponding line integral. Integral forms of the divergence equations of Maxwell (3) and (4) involve surface integrals over the closed surfaces of elementary volume cells.

Discretization of the line integrals is based on the assumption that a field does not vary extensively along a side of a cell in either radial or axial direction, and thus can be approximated as being constant and equal to the field nodal value at the center of that cell side (piecewise-constant approximation). The surface integrals are discretized assuming that the flux densities do not vary over the respective cell faces, in either the radial or the axial direction, but they do vary, in the prescribed harmonic fashion, with the angle of azimuth ϕ.

The curl equation (1) for the shaded electric cell face ($r=$ const "plane") in Fig. 1 can be discretized in the following manner:

$$\begin{aligned}&\Delta zE_z(r,z)\left[\cos(m\phi_0+m\Delta\phi)-\cos(m\phi_0)\right]\\&\quad+r\left[E_\phi(r,z-\Delta z/2)-E_\phi(r,z+\Delta z/2)\right]\\&\quad\cdot\int_{\phi_0}^{\phi_0+\Delta\phi}\sin(m\phi)\,d\phi\\&=-j\omega\Delta z(1/2)\left[\mu(r,z-\Delta z/2)+\mu(r,z+\Delta z/2)\right]\\&\quad\cdot rH_r(r,z)\int_{\phi_0}^{\phi_0+\Delta\phi}\sin(m\phi)\,d\phi.\end{aligned} \quad (9)$$

After the analytic integration has been carried out and the common terms have been canceled, the following expression is obtained:

$$\begin{aligned}&rE_\phi(r,z-\Delta z/2)-rE_\phi(r,z+\Delta z/2)-\Delta zmE_z(r,z)\\&\qquad=-j\omega\Delta zr\mu_r(r,z)H_r(r,z)\end{aligned} \quad (10)$$

where the "averaged" media parameter has been introduced:

$$\mu_r(r,z)=(1/2)\left[\mu(r,z-\Delta z/2)+\mu(r,z+\Delta z/2)\right]. \quad (11)$$

Following the same procedure, the curl equation (1) can be discretized for the electric cell faces in $\phi=$ const and $z=$ const planes.

For $\phi = \text{const}$ planes,

$$\Delta r\left[E_r(r, z+\Delta z/2) - E_r(r, z-\Delta z/2)\right] + \Delta z\left[E_z(r-\Delta r/2, z) - E_z(r+\Delta r/2, z)\right] = -j\omega\Delta r\Delta z\mu_\phi(r, z)H_\phi(r, z). \quad (12)$$

For $z = \text{const}$ planes,

$$\Delta rmE_r(r, z) + (r+\Delta r/2)E_\phi(r+\Delta r/2, z) - (r-\Delta r/2)E_\phi(r-\Delta r/2, z) = -j\omega\Delta rr\mu_z(r, z)H_z(r, z). \quad (13)$$

The discretized equations for the curl equation (2) are obtained by duality, resulting in three additional equations for the components of the magnetic field intensity.

Discretization of the divergence equations requires the expressions for the surface integrals over the six faces of electric and magnetic cells. These integrals have already been obtained for the right-hand sides of the discretized curl equations. Adding them algebraically with the reference direction into the cells, one obtains from divergence equation (3) applied to the magnetic cells

$$m\Delta r\Delta z\epsilon_\phi(r, z)E_\phi(r, z) + \Delta z\left[(r-\Delta r/2)\epsilon_r(r-\Delta r/2, z)\cdot E_r(r-\Delta r/2, z) - (r+\Delta r/2)\epsilon_r(r+\Delta r/2, z)\cdot E_z(r+\Delta r/2, z)\right] + \Delta rr\left[\epsilon_z(r, z-\Delta z/2)\cdot E_z(r, z-\Delta z/2) - \epsilon_z(r, z+\Delta z/2)E_z(r, z+\Delta z/2)\right] = 0. \quad (14)$$

A similar relationship can be obtained for the components of the magnetic field by applying divergence equation (4) to the electric cells. After rearranging, the ϕ-directed field components can be expressed in terms of the radial and axial field components:

$$E_\phi(r, z) = \frac{-1}{m\epsilon_\phi(r, z)}\left[\frac{r-\Delta r/2}{\Delta r}\epsilon_r(r-\Delta r/2, z)\cdot E_r(r-\Delta r/2, z) - \frac{r+\Delta r/2}{\Delta r}\epsilon_r(r+\Delta r/2, z)\cdot E_r(r+\Delta r/2, z) + \frac{r}{\Delta z}\epsilon_z(r, z-\Delta z/2)E_z(r, z-\Delta z/2) - \frac{r}{\Delta z}\epsilon_z(r, z+\Delta z/2)E_z(r, z+\Delta z/2)\right] \quad (15)$$

$$H_\phi(r, z) = \frac{-1}{m\mu_\phi(r, z)}\left[\frac{r-\Delta r/2}{\Delta r}\mu_r(r-\Delta r/2, z)H_r(r-\Delta r/2, z) - \frac{r+\Delta r/2}{\Delta r}\mu_r(r+\Delta r/2, z)H_r(r+\Delta r/2, z) + \frac{r}{\Delta z}\mu_z(r, z-\Delta z/2)H_z(r, z-\Delta z/2) - \frac{r}{\Delta z}\mu_z(r, z+\Delta z/2)H_z(r, z+\Delta z/2)\right]. \quad (16)$$

The physical meaning of the last two equations is that the field components for any given cell are not all independent, and may not be treated as such, if the divergence equations are to be satisfied as well. The above equations are referred to as the zero-divergence condition, since the divergence equations for media free of charges have been used. Imposition of the zero-divergence condition will be accomplished by eliminating the ϕ-directed fields from the curl equations and formulating an algebraic eigenvalue problem in terms of radial and axial field components only. In this manner, the total number of unknowns is reduced by about one third.

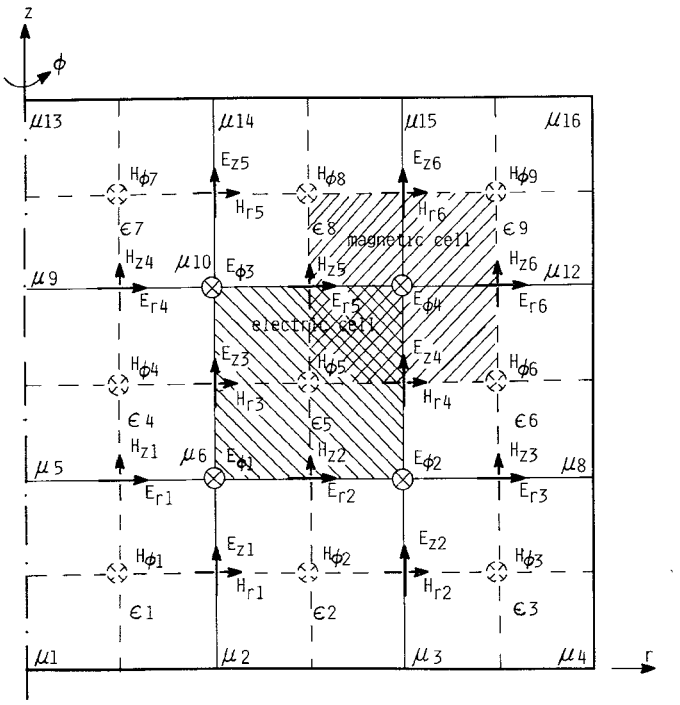

Fig. 2. Discretization of a cavity using (3×3) electric cells. Note that each cell is filled with different dielectrics.

Discretized curl and divergence equations are further simplified if uniform discretization grids are employed: $\Delta r = \Delta z = \Delta l$. Introducing the normalized radial distance $r = r/\Delta l$, and the normalized angular frequency ω_n:

$$\omega_n = \frac{\omega\Delta l}{c} \quad (17)$$

the following identities are obtained:

$$\omega\Delta l\epsilon_0 = \omega_n Y_0 \quad (18)$$

$$\omega\Delta l\mu_0 = \omega_n Z_0 \quad (19)$$

where Z_0 and Y_0 are the intrinsic impedance and admittance of free space.

V. Matrix Formulation

The matrix equations are probably best introduced by means of an example. To this purpose a cylindrical conducting cavity with radius equal to its height, discretized using three electric cells in the radial and three electric

cells in the axial direction, is given in Fig. 2. Each electric or magnetic cell has been assigned a different relative permittivity or permeability. Also indicated in the figure are the positions of the electric and magnetic nodal field components. The boundary conditions on the perfect electric conductor are imposed by setting the tangential electric and normal magnetic field components to zero at the metallic boundaries. The conditions for the field components on the axis of symmetry (z axis) are determined by the field periodicity with the angle of azimuth ϕ. For the modes with $m=0$ (no field variation with ϕ), the r-directed field components on the z axis must be zero, whereas for the modes with $m>0$ the z-directed field components on the z axis must be equal to zero.

Algebraic equations representing the discretization of the curl and divergence equations can be written for this 3×3 cavity as follows. From curl equation (2), for $r=$ const planes, one obtains

$$
\begin{aligned}
(1/2)H_{\phi 4}-(1/2)H_{\phi 1}+mH_{z1} &= j\omega_n Y_0(1/2)\frac{\epsilon_1+\epsilon_4}{2}E_{r1}\\
(3/2)H_{\phi 5}-(3/2)H_{\phi 2}+mH_{z2} &= j\omega_n Y_0(3/2)\frac{\epsilon_2+\epsilon_5}{2}E_{r2}\\
(5/2)H_{\phi 6}-(5/2)H_{\phi 3}+mH_{z3} &= j\omega_n Y_0(5/2)\frac{\epsilon_3+\epsilon_6}{2}E_{r3}\\
(1/2)H_{\phi 7}-(1/2)H_{\phi 3}+mH_{z4} &= j\omega_n Y_0(1/2)\frac{\epsilon_7+\epsilon_4}{2}E_{r4}\\
(3/2)H_{\phi 8}-(3/2)H_{\phi 5}+mH_{z5} &= j\omega_n Y_0(3/2)\frac{\epsilon_8+\epsilon_5}{2}E_{r5}\\
(5/2)H_{\phi 9}-(5/2)H_{\phi 6}+mH_{z6} &= j\omega_n Y_0(5/2)\frac{\epsilon_9+\epsilon_6}{2}E_{r6}.
\end{aligned}
\tag{20}
$$

This system of equations can also be written in the matrix form:

$$
\begin{bmatrix}
-1 & 0 & 0 & 1 & 0 & 0 & 0 & 0 & 0\\
0 & -1 & 0 & 0 & 1 & 0 & 0 & 0 & 0\\
0 & 0 & -1 & 0 & 0 & 1 & 0 & 0 & 0\\
0 & 0 & 0 & -1 & 0 & 0 & 1 & 0 & 0\\
0 & 0 & 0 & 0 & -1 & 0 & 0 & 1 & 0\\
0 & 0 & 0 & 0 & 0 & -1 & 0 & 0 & 1
\end{bmatrix}
\cdot
\begin{bmatrix}
1/2 & 0 & 0 & 0 & 0 & 0 & 0 & 0 & 0\\
0 & 3/2 & 0 & 0 & 0 & 0 & 0 & 0 & 0\\
0 & 0 & 5/2 & 0 & 0 & 0 & 0 & 0 & 0\\
0 & 0 & 0 & 1/2 & 0 & 0 & 0 & 0 & 0\\
0 & 0 & 0 & 0 & 3/2 & 0 & 0 & 0 & 0\\
0 & 0 & 0 & 0 & 0 & 5/2 & 0 & 0 & 0\\
0 & 0 & 0 & 0 & 0 & 0 & 1/2 & 0 & 0\\
0 & 0 & 0 & 0 & 0 & 0 & 0 & 3/2 & 0\\
0 & 0 & 0 & 0 & 0 & 0 & 0 & 0 & 5/2
\end{bmatrix}
\cdot
\begin{bmatrix}
H_{\phi 1}\\ H_{\phi 2}\\ H_{\phi 3}\\ H_{\phi 4}\\ H_{\phi 5}\\ H_{\phi 6}\\ H_{\phi 7}\\ H_{\phi 8}\\ H_{\phi 9}
\end{bmatrix}
+m
\begin{bmatrix}
H_{z1}\\ H_{z2}\\ H_{z3}\\ H_{z4}\\ H_{z5}\\ H_{z6}
\end{bmatrix}
=j\omega_n Y_0
\begin{bmatrix}
1/2 & 0 & 0 & 0 & 0 & 0\\
0 & 3/2 & 0 & 0 & 0 & 0\\
0 & 0 & 5/2 & 0 & 0 & 0\\
0 & 0 & 0 & 1/2 & 0 & 0\\
0 & 0 & 0 & 0 & 3/2 & 0\\
0 & 0 & 0 & 0 & 0 & 5/2
\end{bmatrix}
$$

$$
\cdot
\begin{bmatrix}
(\epsilon_1+\epsilon_4)/2 & 0 & 0 & 0 & 0 & 0\\
0 & (\epsilon_2+\epsilon_5)/2 & 0 & 0 & 0 & 0\\
0 & 0 & (\epsilon_3/\epsilon_6)/2 & 0 & 0 & 0\\
0 & 0 & 0 & (\epsilon_4+\epsilon_7)/2 & 0 & 0\\
0 & 0 & 0 & 0 & (\epsilon_5+\epsilon_8)/2 & 0\\
0 & 0 & 0 & 0 & 0 & (\epsilon_6+\epsilon_9)/2
\end{bmatrix}
\begin{bmatrix}
E_{r1}\\ E_{r2}\\ E_{r3}\\ E_{r4}\\ E_{r5}\\ E_{r6}
\end{bmatrix}.
\tag{21}
$$

In a compact notation, (21) becomes

$$\boldsymbol{C}^h_{\phi r}\boldsymbol{D}^h_{r\phi}|h_\phi\rangle + m|h_z\rangle = j\omega_n Y_0 \boldsymbol{D}^e_{rr}\boldsymbol{D}_{\epsilon r}|e_r\rangle \tag{22}$$

where the boldface symbols denote square or rectangular matrices with real elements, and the symbol $|\ \rangle$ denotes column matrices with real elements. Likewise, the curl equation (2), written for $\phi = \text{const}$ and $z = \text{const}$ planes, results in

$$\boldsymbol{C}^h_{r\phi}|h_r\rangle + \boldsymbol{C}^h_{z\phi}|h_z\rangle = j\omega_n Y_0 \boldsymbol{D}_{\epsilon\phi}|e_\phi\rangle \tag{23}$$

$$-m|h_r\rangle + \boldsymbol{C}^h_{\phi z}\boldsymbol{D}^h_{r\phi}|h_\phi\rangle = j\omega_n Y_0 \boldsymbol{D}^e_{rz}\boldsymbol{D}_{\epsilon z}|e_z\rangle. \tag{24}$$

Proceeding in an analogous manner, curl equation (1) results in

$$\boldsymbol{C}^e_{\phi r}\boldsymbol{D}^e_{r\phi}|e_\phi\rangle - m|e_z\rangle = -j\omega_n Z_0 \boldsymbol{D}^h_{rr}\boldsymbol{D}_{\mu r}|h_r\rangle \tag{25}$$

$$\boldsymbol{C}^e_{r\phi}|e_r\rangle + \boldsymbol{C}^e_{z\phi}|e_z\rangle = -j\omega_n Z_0 \boldsymbol{D}_{\mu\phi}|h_\phi\rangle \tag{26}$$

$$m|e_r\rangle + \boldsymbol{C}^e_{\phi z}\boldsymbol{D}^e_{r\phi}|e_\phi\rangle = -j\omega_n Z_0 \boldsymbol{D}^h_{rz}\boldsymbol{D}_{\mu z}|h_z\rangle. \tag{27}$$

Three classes of matrices are recognized in (22) to (27): connection matrices $\boldsymbol{C}^*_{**}$, representing the discretization of line integrals; diagonal position matrices $\boldsymbol{D}^*_{**}$, representing the radial distances of nodal field components; and diagonal media matrices $\boldsymbol{D}_{**}$, representing the averaging of media parameters for adjacent cells involved in discretization of surface integrals.

In an analogous manner, the divergence equations (3) and (4) result in the following two matrix equations:

$$m\boldsymbol{D}_{\epsilon\phi}|e_\phi\rangle + \boldsymbol{C}^e_{rd}\boldsymbol{D}^e_{rr}\boldsymbol{D}_{\epsilon r}|e_r\rangle + \boldsymbol{C}^e_{zd}\boldsymbol{D}^e_{rz}\boldsymbol{D}_{\epsilon z}|e_z\rangle = 0 \tag{28}$$

$$m\boldsymbol{D}_{\mu\phi}|h_\phi\rangle + \boldsymbol{C}^h_{rd}\boldsymbol{D}^h_{rr}\boldsymbol{D}_{\mu r}|h_r\rangle + \boldsymbol{C}^h_{zd}\boldsymbol{D}^h_{rz}\boldsymbol{D}_{\mu z}|h_z\rangle = 0. \tag{29}$$

For cavities which do not contain magnetic materials, the media matrices $\boldsymbol{D}_{\mu r}$ and $\boldsymbol{D}_{\mu z}$ are replaced by the scalar μ_0. Likewise, for the air-filled cavities, $\boldsymbol{D}_{\epsilon r}$ and $\boldsymbol{D}_{\epsilon z}$ are replaced by ϵ_0. The connection matrices for the divergence equations are related to the connection matrices for the curl equations, as shown in [11]. The example in Fig. 2 there are only (3×3) electric cells, but any larger number of cells can obviously be formulated in like manner, resulting in matrix equations of the same form as (22) to (29).

VI. Eigenvalue Problem Formulation

The first step toward the electric field formulation is to express the magnetic field vectors in terms of vectors of electric field components, from equations (25) to (27):

$$|h_r\rangle = \frac{-1}{j\omega_n Z_0}\boldsymbol{D}^{-1}_{\mu r}\left(\boldsymbol{D}^h_{rr}\right)^{-1}\left[\boldsymbol{C}^e_{\phi r}\boldsymbol{D}^e_{r\phi}|e_\phi\rangle - m|e_z\rangle\right] \tag{30}$$

$$|h_\phi\rangle = \frac{-1}{j\omega_n Z_0}\boldsymbol{D}^{-1}_{\mu\phi}\left[\boldsymbol{C}^e_{r\phi}|e_r\rangle + \boldsymbol{C}^e_{z\phi}|e_z\rangle\right] \tag{31}$$

$$|h_z\rangle = \frac{-1}{j\omega_n Z_0}\boldsymbol{D}^{-1}_{\mu z}\left(\boldsymbol{D}^h_{rz}\right)^{-1}\left[m|e_r\rangle + \boldsymbol{C}^e_{\phi z}\boldsymbol{D}_{r\phi}|e_\phi\rangle\right]. \tag{32}$$

The above is next substituted into (23) and (24). The resulting expressions involve the vector of ϕ-directed electric field components, which can be expressed, from the zero-divergence condition (28), in terms of the radial and axial electric field vectors to give the following partitioned matrix equation:

$$\left\{\begin{bmatrix}\boldsymbol{A}^e_{rr} & \boldsymbol{A}^e_{rz}\\ \boldsymbol{A}^e_{zr} & \boldsymbol{A}^e_{zz}\end{bmatrix} - \omega_n^2\begin{bmatrix}\boldsymbol{D}^e_{rr}\boldsymbol{D}_{\epsilon r} & \boldsymbol{0}\\ \boldsymbol{0} & \boldsymbol{D}^e_{rz}\boldsymbol{D}_{\epsilon z}\end{bmatrix}\right\}\begin{bmatrix}|e_r\rangle\\ |e_z\rangle\end{bmatrix} = 0. \tag{33}$$

Matrices $\boldsymbol{A}^e_{**}$ are defined as follows:

$$\boldsymbol{A}^e_{rr} = \boldsymbol{C}^h_{\phi r}\boldsymbol{D}^h_{r\phi}\boldsymbol{D}^{-1}_{\mu\phi}\boldsymbol{C}^e_{r\phi} + m^2\boldsymbol{D}^{-1}_{\mu z}\left(\boldsymbol{D}^h_{rz}\right)^{-1} - \omega_n^2\boldsymbol{D}^e_{rr}\boldsymbol{D}_{\epsilon r} \tag{34}$$

$$\boldsymbol{A}^e_{rz} = \boldsymbol{C}^h_{\phi r}\boldsymbol{D}^h_{r\phi}\boldsymbol{D}^{-1}_{\mu\phi}\boldsymbol{C}^e_{z\phi} \tag{35}$$

$$\boldsymbol{A}^e_{zr} = \boldsymbol{C}^h_{\phi z}\boldsymbol{D}^h_{r\phi}\boldsymbol{D}^{-1}_{\mu\phi}\boldsymbol{C}^e_{r\phi} \tag{36}$$

$$\boldsymbol{A}^e_{zz} = \boldsymbol{C}^h_{\phi z}\boldsymbol{D}^h_{r\phi}\boldsymbol{D}^{-1}_{\mu\phi}\boldsymbol{C}^e_{z\phi} + m^2\boldsymbol{D}^{-1}_{\mu r}\left(\boldsymbol{D}^h_{rr}\right)^{-1} - \omega_n^2\boldsymbol{D}^e_{rz}\boldsymbol{D}_{\epsilon z}. \tag{37}$$

Equation (33) is recognized as the standard eigenvalue problem if written in one of the following forms:

$$\left[\boldsymbol{A}^e - \omega_n^2\boldsymbol{D}^e\right]|e_{rz}\rangle = 0 \tag{38}$$

or

$$\left[\left(\boldsymbol{D}^e\right)^{-1}\boldsymbol{A}^e - \omega_n^2\boldsymbol{I}\right]|e_{rz}\rangle = 0. \tag{39}$$

The resulting matrix is very sparse, with at most nine elements per row, regardless of the matrix size.

A dual procedure can be carried out for the magnetic field formulation. The result is a standard algebraic eigenvalue problem of the form

$$\left[\boldsymbol{A}^h - \omega_n^2\boldsymbol{D}^h\right]|h_{rz}\rangle = 0 \tag{40}$$

or

$$\left[\left(\boldsymbol{D}^h\right)^{-1}\boldsymbol{A}^h - \omega_n^2\boldsymbol{I}\right]|h_{rz}\rangle = 0. \tag{41}$$

The two eigenvalue problem formulations for $m > 0$ modes are redundant, in the sense that the curl and divergence equations can be used to recover all of the field vectors once either radial and axial electric or radial and axial magnetic eigenvectors have been obtained.

An eigenvalue formulation for the modes with no field variation along the angle of azimuth ϕ (modes with $m = 0$) can be obtained from the curl equations only, without use of the zero divergence condition. The TE_0 cavity modes are obtained from the following eigenvalue problem:

$$\left[\boldsymbol{A}^e_0 - \omega_n^2\boldsymbol{I}\right]|e_\phi\rangle = 0 \tag{42}$$

with matrix $\boldsymbol{A}^e_0$ given by

$$\boldsymbol{A}^e_0 = \boldsymbol{D}^{-1}_{e\phi}\boldsymbol{C}^h_{r\phi}\boldsymbol{D}^{-1}_{\mu r}\left(\boldsymbol{D}^h_{rr}\right)^{-1}\boldsymbol{C}^e_{\phi r}\boldsymbol{D}^e_{r\phi} + \boldsymbol{D}^{-1}_{\epsilon\phi}\boldsymbol{C}^h_{z\phi}\boldsymbol{D}^{-1}_{\mu z}\left(\boldsymbol{D}^h_{rz}\right)^{-1}\boldsymbol{C}^e_{\phi z}\boldsymbol{D}_{r\phi}. \tag{43}$$

A dual procedure yields the eigenvalue formulation for the TM_0 modes:

$$\left[\boldsymbol{A}^h_0 - \omega_n^2\boldsymbol{I}\right]|h_\phi\rangle = 0 \tag{44}$$

$$\boldsymbol{A}^h_0 = \boldsymbol{D}^{-1}_{\mu\phi}\boldsymbol{C}^e_{r\phi}\boldsymbol{D}^{-1}_{\epsilon z}\left(\boldsymbol{D}^e_{rr}\right)^{-1}\boldsymbol{C}^h_{\phi r}\boldsymbol{D}^h_{r\phi} + \boldsymbol{D}^{-1}_{\mu\phi}\boldsymbol{C}^e_{z\phi}\boldsymbol{D}^{-1}_{\epsilon z}\left(\boldsymbol{D}^h_{rz}\right)^{-1}\boldsymbol{C}^h_{\phi z}\boldsymbol{D}^h_{r\phi}. \tag{45}$$

Therefore for a given number of nodes in a particular cavity, modes with $m = 0$ are obtained by solving a matrix of half smaller size than the one for mode with $m > 0$.

TABLE I
NUMBER OF ELEMENTS IN THE FIELD EIGENVECTORS, WHERE M IS THE NUMBER OF RADIAL CELLS AND N IS THE NUMBER OF AXIAL CELLS

	m = 0 modes	m > 0 modes
$\|e_r\rangle$	M(N - 1)	M(N - 1)
$\|e_\phi\rangle$	(M - 1)(N - 1)	(M - 1)(N - 1)
$\|e_z\rangle$	MN	(M - 1)N
$\|h_r\rangle$	(M - 1)N	MN
$\|h_\phi\rangle$	MN	MN
$\|h_z\rangle$	M(N - 1)	M(N - 1)

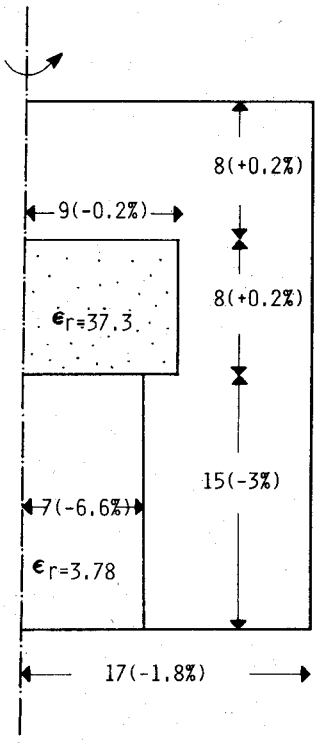

Fig. 3. Discretization of the cavity used in experiments, and the corresponding percentage errors.

To illustrate the size of the resulting matrix problem, we consider a cavity with M electric cells in the radial direction and N cells in the axial direction. The corresponding number of elements for the electric and magnetic field vectors is given in Table I. For the example from Fig. 3, $M=17$ and $N=31$, $|e_\phi\rangle$ vector has 480 components, so that the matrix which must be solved in the case of the TE_0 modes is 480×480. For any of the hybrid modes with $m>0$, the matrix size for the same cavity increases to 1037×1037.

When the numerical solution of the eigenvalue problem has been obtained, the eigenvalues yield the resonant frequencies of the modes, and the eigenvectors contain the r and z components of the field. Typically, only the lowest five to ten modes for each m are of practical interest.

The field lines of the various resonant modes are plotted on an $x-y$ plotter controlled by a personal computer using the procedure described in [12]. Knowledge of the field distribution in the cavity allows a detailed computation of the unloaded Q factor, taking into account the dielectric losses as well as metal wall losses.

VII. Mode Nomenclature

The eigenvalue formulation inherent in the finite integration technique provides an opportunity of a mode nomenclature for resonant cavities with rotational symmetry, containing the dielectric resonators, in a straightforward way. Until now, a number of authors have attempted miscellaneous notations, but none have been generally accepted. For hybrid modes ($m>0$), the disagreement is the most noticeable. The letters used by various authors to denote these resonant modes are EH and HE [13], [14]; TE_D, TE_H, TM_D, and TM_H [15]; HEM [16]; and HEH and HEE [17]. The subscripts are usually two integers followed by symbol the δ [16], [18] or p [2], but also fractions [13], and combination of three integer subscripts plus three integer superscripts [14] have been used. The only feature common to all these notations is that the first subscript is used to denote m, the azimuthal variation number from (7) and (8).

The presence of several dielectric regions such as air, dielectric resonator, support, and tuning objects makes the field distribution too complicated for a complete description in terms of three indices. For example, the field plots of the lowest five TM_0 modes in the shielded dielectric resonator [19] show that any use of three indices leads to contradictions, even for the relatively simple $m=0$ case.

It appears that a simple solution to this dilemma is using only two integer indices instead, as first proposed in [5] and [17]. The first index should be the azimuthal modal index m; the second index, n, should be an integer, starting with $n=1$ and counting the resonant frequencies of various modes in ascending order for the specified value of m. When the frequencies are obtained from an eigenvalue problem, such as in the FIT, the eigenvalues are already arranged in ascending order by computer, and the numbering is unambiguous.

As far as the choice of letters is concerned, the controversy stems largely from the dual meaning of the letter H. Some use "H" to denote the hybrid modes, others use it to denote the transverse electric modes. The controversy can be avoided if one returns to the original IRE standard [20], which classifies four categories of guided waves: TEM (transverse electromagnetic), TE (transverse electric), TM (transverse magnetic), and HEM (hybrid electromagnetic). Applied to the rotational cavities containing dielectric resonators, the resonant modes should thus be denoted TE_{0n}, TM_{0n}, and HEM_{mn}.

VIII. Solution Examples

The cavity from Fig. 3 was analyzed by FIT using a uniform grid of 17×31 nodes, the grid step being 0.427 mm. The geometrical errors due to the finite grid discretization are also indicated in the figure. Eigensolutions for the TE and TM modes, and the HEM modes with $m=1$, 2, and 3, have been obtained. The same cavity was

TABLE II
MEASURED AND COMPUTED RESONANT FREQUENCIES OF THE CAVITY IN FIG. 4

	Frequency in GHz		Relative
	Computed	Measured	Error in %
TE_{01}	7.037	6.943	+1.35
HEM_{11}	8.742	8.694	+0.55
HEM_{12}	8.897	8.905	-0.09
TM_{01}	9.296	9.185	+1.21
HEM_{21}	10.605	10.558	+0.45
TM_{02}	11.113	10.943	+1.55
HEM_{13}	11.226	11.184	+0.38
TE_{02}	11.391	11.316	+0.66

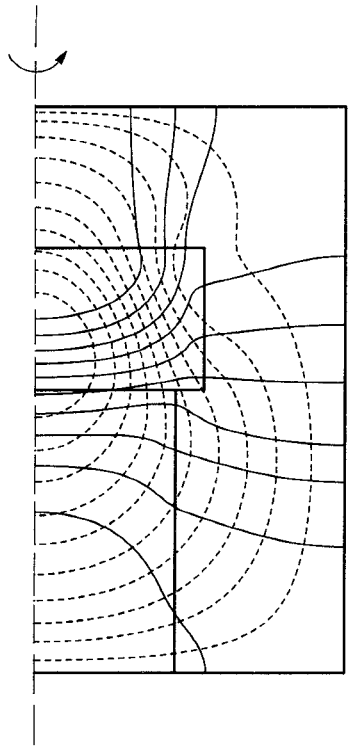

Fig. 4. Electric (solid) and magnetic (dashed) field lines for the HEM_{11} mode in the cavity of Fig. 4.

then measured using a HP8410A network analyzer and a HP8672A synthesized signal generator. The predicted and measured resonant frequencies, and their relative differences, are given in Table II. The predicted and measured resonant frequencies of the lowest 12 resonant modes agree within 1.5 percent. Taking into account that the cavity coupling mechanism distorts the rotational shape and that the discretization error of certain dimensions in Fig. 3 is as high as 6 percent, the difference can be mainly attributed to the imperfections of the experimental, rather than numerical, model.

The sample field distributions for the hybrid modes in this cavity are given in Figs. 4 and 5. It may be noted that the electric field lines do not show sudden change of direction at the interfaces of different dielectric materials,

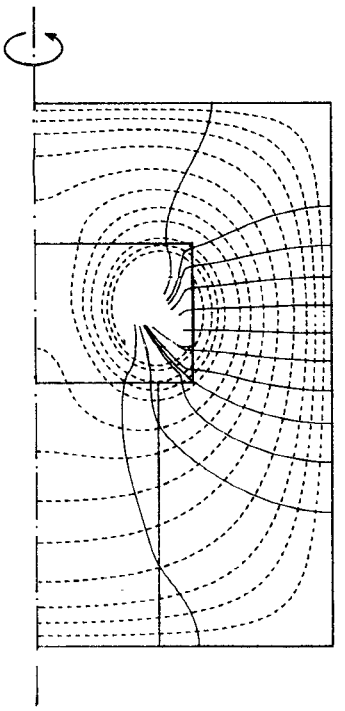

Fig. 5. Electric (solid) and magnetic (dashed) field lines for the HEM_{13} mode in the cavity of Fig. 4. Note the spiraling behavior of the field inside the dielectric resonator.

but rather a gradual change. The reason for this behavior is the finite size of the discretization grid utilized in the solution. The computer-generated field plots are constructed by using the second-order Runge–Kutta procedure, whereas the local field inclination is obtained by interpolating between nearest data points [12]. Therefore, one cannot expect the field lines to display a sudden change of direction within a distance smaller than the cell size Δ. In order to obtain a sharper transition in the field line directions, one would have to decrease the cell size, with the consequence of increasing the matrix size, and therefore increasing the computer time needed for obtaining the eigensolutions.

An unusual modal field pattern can be seen in Fig. 5, which depicts the mode HEM_{13}. The field lines of this mode exhibit localized spiraling behavior within the dielectric resonator. Such behavior cannot be found in the cavities filled with homogeneous dielectrics, and it appears to be a novel phenomenon, related to the inhomogeneity of the dielectric material within the cavity. The same HEM_{13} pattern has been obtained using the magnetic field and the electric field FIT formulations, the two being entirely different matrix generation procedures, so that it is believed to be correct.

The computation of the unloaded Q factor, including both dielectric and conductor losses, is straightforward, because the eigenvectors of each mode contain information on the field distribution within the cavity. The entire loss is obtained by numerical integration over the cavity volume and surface. A verification of the procedure is next described for a hollow cylindrical cavity of radius 5 cm and

height 7 cm. Assuming a copper conductivity of $5.8 \cdot 10^7$ S/m, the theoretical resonant frequency of the mode TE_{111} is expected to be 2.77184 GHz [7, p. 214], and the conductor Q factor to be $Q_c = 23787$ [7, p. 257]. Using the square grid with 10×14 elements of size 5 mm, the resonant frequency obtained by the FIT is 2.76839 GHz and the corresponding $Q_c = 24605$. Therefore, even with such a small number of cells, the FIT provides a 0.1 percent accuracy for resonant frequency and a 3 percent accuracy for Q_c factor.

IX. Conclusion

The finite integration technique (FIT) has been employed for the numerical solution of rotationally symmetric cavities containing dielectric resonators. The eigen solution of the matrix provides the resonant frequencies and the associated field distributions for a prescribed azimuthal modal number m. As the eigenvalues are arranged in ascending order, the numbering of the eigenvalues can be conveniently used as the second subscript of the modal nomenclature. The modes are therefore denoted as TE_{0n}, TM_{0n}, and HEM_{mn}.

The matrix eigenvectors are used as input data for computer-generated modal field patterns, enabling one to identify the regions of strong or weak field and predict the coupling or tuning effects. Unloaded Q factors have also been evaluated, indicating the individual contributions of losses in the metal and the dielectric to the overall Q factors.

In comparison with the commonly used mode-matching numerical procedures, the FIT offers the following advantages: (1) the matrix elements are independent of frequency; (2) the matrix elements do not contain any higher functions (such as Bessel functions); (3) no axial symmetry in the cavity is required, and (4) no prior knowledge of regional modes (e.g. complex modes) is required, so that the possibility of missing any resonances is reduced. The drawbacks of the FIT are: (1) the need of handling large sparse matrices and (2) the fact that in the present formulation the matrix is not symmetric and not banded, which slows down the numerical eigensolution procedure. Future efforts will be directed toward alleviating the latter inconvenience [21].

Acknowledgment

The authors are indebted to J. A. Gerald, Syracuse University (formerly with the Department of Electrical Engineering, University of Mississippi), for preparation of BASIC programs for graphical display of the computed fields. The verification of the Q factor accuracy was performed by W. L. Wu, Department of Electrical Engineering, University of Mississippi.

References

[1] K. A. Michalski, "Rigorous analysis methods," ch. 5 in *Dielectric Resonators*. Norwood, MA: Artech House, 1986.

[2] P. Guillon, J. P. Balabaud, and Y. Garault, "TM_{01p} tubular and cylindrical dielectric resonator mode," in *IEEE MTT-S Int. Microwave Symposum Dig.* (Los Angeles, CA), June 15–19, 1981, pp. 163–166.

[3] M. Albani and P. Bernardi, "A numerical method based on the discretization of Maxwell's equations in integral form," *IEEE Trans. Microwave Theory Tech.*, vol. MTT-24, pp. 446–449, Apr. 1974.

[4] T. Weiland, "Eine Methode zur Loesung der Maxwellschen Gleichungen fuer sechskomponentinge Felder auf diskreter Basis," *Arch. Elek. Übertragung.*, vol. 31, pp. 116–120, 1977.

[5] T. Weiland, "On the computation of resonant modes in cylindrically symmetric cavities," *Nucl. Instrum. Methods*, vol. 216, pp. 329–348, 1983.

[6] U. van Rienen and T. Weiland, "Triangular discretization method for the evaluation of rf-fields in cylindrical.ly symmetric cavities," *IEEE Trans. Magn.*, vol. MAG-21, pp. 2317–2320, Nov. 1985.

[7] R. F. Harrington, *Time Harmonic Electromagnetic Field*. New York: McGraw-Hill, 1965.

[8] A. J. Kobelansky and J. P. Webb, "Eliminating spurious modes in finite-element waveguide problems by using divergence-free fields," *Electron. Lett.*, vol. 22, no. 11, pp. 569–570, 1986.

[9] K. A. Zaki and C. Chen, "Complex modes in dielectric loaded waveguides," in *IEEE AP-S Int. Symposium Dig.*, June 1987, pp. 8–11.

[10] K. S. Yee, "Numerical solution of initial boundary value problems involving Maxwell's equations in isotropic media," *IEEE Trans. Antennas Propag.*, vol. AP-14, pp. 302–307, 1966.

[11] J. Lebaric, "Study of inhomogeneously filled cylindrical resonant cavities by the finite integration technique," Ph.D. Dissert., U. of Mississippi, Nov. 1987, *University Microfilms International*, No. 88-04282.

[12] D. Kajfez and J. A. Gerald, "Plotting of vector fields with personal computer," *IEEE Trans. Microwave Theory Tech.*, vol. MTT-35, pp. 1069–1072, Nov. 1987.

[13] Y. Kobayashi, N. Fukuoka, and S. Yoshida, "Resonant modes for a shielded dielectric rod resonator," *Electron. and Commun. Japan*, vol. 64-B, no. 11, pp. 46–51, 1981.

[14] U. Crombach and R. Michelfeit, "Resonanzfrequenzen und Feldstaerken in geschirmten dielektrischen Scheiben- und Ringresonatoren," *Frequenz*, vol. 35, no. 12, pp. 324–328, 1981.

[15] U. S. Hong and R. H. Jansen, "Veraenderung der Resonanzfrequenzen dielektrischer Resonatoren in Mikrostripschaltungen durch Umgebungsparameter," *Arch. Elek. Übertragung.*, vol. 38, pp. 106–112, 1984.

[16] A. W. Glisson, D. Kajfez and J. James, "Evaluation of modes in dielectric resonators using a surface integral equation formulation," *IEEE Trans. Microwave Theory Tech.*, vol. MTT-31, pp. 1023–1029, Dec. 1983.

[17] K. A. Zaki and C. Chen, "New results in dielectric-loaded resonators, *IEEE Trans. Microwave Theory Tech.*, vol. MTT-34, pp. 815–824, July 1986.

[18] Y. Konishi, N. Hoshino, and Y. Utsumi, "Resonant frequency of a $TE_{01\delta}$ dielectric resonator," *IEEE Trans. Microwave Theory Tech.*, vol. MTT-24, pp. 112–114, Feb. 1976.

[19] D. Kajfez and J. Lebaric, "Field patterns of TM_0 modes in a shielded dielectric resonator," *Electron. Lett.*, vol. 23, pp. 944–946, Aug. 27, 1987.

[20] "IRE standards on antennas and waveguides: definitions of terms, 1953," *Proc. IRE*, vol. 41, pp. 1721–1728, Dec. 1953.

[21] T. Okada and D. Kajfez, "FIT formulation for cylindrical cavities resulting in a symmetric matrix," in *Proc. 1989 URSI EM Theory Symp.* (Stockholm, Sweden), Aug. 14–17, 1989, pp. 332–334.

✠

Jovan E. Lebaric (S'84'–M'87) was born in Novi Sad, Yugoslavia, in 1952. He attended the University of Belgrade, Belgrade, Yugoslavia, and received the Diploma in electrical engineering in 1976. In 1983 he received the M.S. degree in electrical engineering, also from the University of Belgrade. From 1983 to 1987 he attended the University of Mississippi, University, MS, where he earned the Ph.D. degree in electrical engineering in 1987.

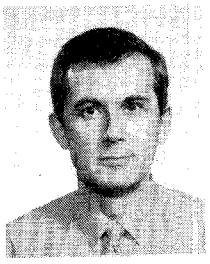

He was an Instructor in Electrical Engineering at The University of Mississippi from 1984 to 1987. Since 1987 he has been with the Rose–Hulman Institute of Technology, Terre Haute, IN, as visiting Assistant Professor of Electrical and Computer Engineering teaching courses in electromagnetics and communications. His main research interests are in applied computational electromagnetics, methods for direct solution of Maxwell's equations, supercomputing applications in electromagnetics, and software development for the solution of interior and exterior electromagnetic boundary value problems.

Dr. Lebaric is an IEEE student branch counselor at the Rose–Hulman Institute of Technology, a member of the Applied Computational Electromagnetics Society (ACES), and a member of Sigma Xi.

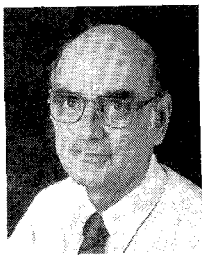

Darko Kajfez (SM'67) obtained the electrical engineer's degree (Dipl. Ing.) from the University of Ljubljana, Yugoslavia, in 1953 and the Ph.D. degree from the University of California, Berkeley, in 1967.

He is a professor of electrical engineering at the University of Mississippi. His teaching and research interests are in application of electromagnetic theory in microwave circuits and antennas.

Dr. Kajfez coedited the book *Dielectric Resonators* and authored three volumes of the graduate textbook *Notes on Microwave Circuits*.